

CrystEngComm

Accepted Manuscript



This is an *Accepted Manuscript*, which has been through the Royal Society of Chemistry peer review process and has been accepted for publication.

Accepted Manuscripts are published online shortly after acceptance, before technical editing, formatting and proof reading. Using this free service, authors can make their results available to the community, in citable form, before we publish the edited article. We will replace this *Accepted Manuscript* with the edited and formatted *Advance Article* as soon as it is available.

You can find more information about *Accepted Manuscripts* in the [Information for Authors](#).

Please note that technical editing may introduce minor changes to the text and/or graphics, which may alter content. The journal's standard [Terms & Conditions](#) and the [Ethical guidelines](#) still apply. In no event shall the Royal Society of Chemistry be held responsible for any errors or omissions in this *Accepted Manuscript* or any consequences arising from the use of any information it contains.

ARTICLE

Self-assembly and Magnetic Properties of Ni(II)/Co(II) Coordination Polymers Based on 1,4-Bis(imidazol-1-yl)benzene and Varying Biphenyltetracarboxylates

Cite this: DOI: 10.1039/x0xx00000x

Feng Su^a, Liping Lu^{*a}, Sisi Feng^a, and Miaoli Zhu^{*a,b}

Received 00th January 2012,

Accepted 00th January 2012

DOI: 10.1039/x0xx00000x

www.rsc.org/

Solvothermal or hydrothermal methods of $M(\text{NO}_3)_2 \cdot 6\text{H}_2\text{O}$ ($M = \text{Ni}(\text{II})$ or $\text{Co}(\text{II})$) with N-donor (1,4-bis(imidazol-1-yl)benzene, 1,4-bib) and auxiliary deprotonated biphenyltetracarboxylates (2,2',5,5'-biphenyltetracarboxylic acid, $\text{H}_4(\text{o,m-bpta})$; 3,3',5,5'-biphenyltetracarboxylic acid, $\text{H}_4(\text{m,m-bpta})$; or 3,3',4,4'-biphenyltetracarboxylic acid, $\text{H}_4(\text{m,p-bpta})$) give five novel coordination polymers in H_2O -DMF or H_2O , namely, $[\text{Ni}_2(1,4\text{-bib})_3(\text{o,m-bpta})(\text{H}_2\text{O})_2]$ (**1**), $[\text{Ni}_2(1,4\text{-bib})_3(\text{HCO}_2)_4(\text{H}_2\text{O})_2] \cdot 5\text{H}_2\text{O}$ (**2**), $[\text{Co}_2(1,4\text{-bib})_2(\text{m,m-bpta})(\text{H}_2\text{O})_4]$ (**3**), $[\text{Ni}_2(1,4\text{-bib})_2(\text{m,p-bpta})(\text{H}_2\text{O})_2]$ (**4**) and $[\text{Co}_2(1,4\text{-bib})_2(\text{m,p-bpta})(\text{H}_2\text{O})_2]$ (**5**). The structural messages of the complexes have been acquired by single-crystal XRD data and further characterized by EA, IR spectra, powder XRD and TG analysis. The framework of **1** is constructed by a 3D interpenetration structure with a $(4.6^2)_2(4^2.6^2.8^2)$ topology. Complex **2** exhibits a 3D supramolecular framework assembled by 1D mutual interpenetration chains. Complex **3** generates a 3D supramolecular architecture from (4,4)-connected 2D layers. Complexes **4** and **5** are isomorphism, having 2D sheet structures with (4,4)-grid units. These results reveal that 1,4-bib ligand cooperating with different biphenyltetracarboxylic acids can be used as versatile building blocks for the construction of metal-organic frameworks. Magnetic susceptibility measurements indicate the presence of weak ferromagnetic exchanges between adjacent Ni(II) ions with $g = 2.235(5)$, $2.223(7)$ and $J = 0.906(1)$, $2.220(1) \text{ cm}^{-1}$ for **1** and **4**, respectively.

Introduction

A rapid expansion has been realized in the synthesis, structural characterization, and application of materials known as metal-organic frameworks (MOFs) during the past decades.¹ MOFs have emerged as an extensive class of crystalline materials not only because of their intriguing architectures and topological structures² but also for their potential applications in the areas of catalysis³, gas adsorption⁴, nonlinear optics⁵, magnetism materials⁶, and other possible applications.⁷ So far, impressive progress has been made on the theoretical forecasts and practical approaches of relationship between the structures and

hydrogen bond interaction⁹. The main emphasis on the principle of design is to search for good bridging ligands that can effectively mediate the magnetic coupling between the local spin carriers. whereas magnetic susceptibility measurements can help to elucidate the connectivity between the metal centers.¹⁰

Ligands containing polycarboxylates have been the most widely used as linkers of metal ions in the design of polynuclear complexes with interesting magnetic properties.^{4a,5b,10b,11-13} Some of them, biphenyl-tetracarboxylic acids (H_4bptas) with C_2 symmetry have recently attracted attention owing to their advantageous supramolecular self-assembly and complexation of metal ions.¹⁴ Biphenyltetra-carboxylic acid have distinctive features, such as (i) due to availability of more coordination sites, they can bond to a great number of metal ions¹⁵, thereby forming layer structures and interpenetration structures; (ii) the carboxylic groups can assume many kinds of bridging or multitooth chelating modes to construct rich and colorful MOFs; and (iii) they can act as hydrogen-bond acceptors or donors to form supramolecular structures by hydrogen bonding interactions.^{6a,16} Remarkably, a series of metal-organic structural motifs, including bilayer, ladder,

^aInstitute of Molecular Science, Key Laboratory of Chemical Biology and Molecular Engineering of the Education Ministry, Shanxi University, Taiyuan, Shanxi 030006, P. R. China.

^bState Key Laboratory of Coordination Chemistry, Nanjing University, Nanjing 210093, P. R. China.

Institute of Molecular Science, Shanxi University, 92 Wucheng Road, Taiyuan, Shanxi 030006, P. R.China. Tel: ++86-351-7017974; Fax: ++86-351-7011022; E-mail: luliping@sxu.edu.cn, miaoli@sxu.edu.cn

properties of metal-organic frameworks.⁸ For instance, the magnetic properties of MOFs are greatly affected due to influences of the metal assemblies, the bridging ligands and

hexagonal nanotube, rod, and hourglass, have been deliberately designed by employing bridging biphenyl polycarboxylate.^{16b,17-19} Searching for new linkers forming chain, network, or interpenetrating structural complexes and predicting magnetic properties is still a challenge in the fields of molecular magnetism and crystal engineering.

1,4-Bis(imidazol-1-yl)benzene (1,4-bib, Scheme 1) with C_2 symmetry is a N-donor rigid ligand, which makes a space of 13–14 Å between two metal ions.²⁰ Thus, these considerations inspired us to explore new metal–organic frameworks of 1,4-bib with 2,2',5,5'-biphenyl-tetracarboxylic acid ($H_4(o,m\text{-bpta})$, Scheme 1), 3,3',5,5'-biphenyltetra-carboxylic acid ($H_4(m,m\text{-bpta})$, Scheme 1), and 3,3',4,4'-biphenyltetra-carboxylic acid ($H_4(m,p\text{-bpta})$, Scheme 1) ligands in the presence of metal ions. Herein, the self-assembly of five coordination polymers, namely, $[Ni_2(1,4\text{-bib})_3(o,m\text{-bpta})(H_2O)_2]$ (**1**), $[Ni_2(1,4\text{-bib})_3(HCO_2)_4(H_2O)_2] \cdot 5H_2O$ (**2**), $[Co_2(1,4\text{-bib})_2(m,m\text{-bpta})(H_2O)_4]$ (**3**), and $[M_2(1,4\text{-bib})_2(m,p\text{-bpta})(H_2O)_2]$ ((**4**) M = Ni, and (**5**) M = Co) is reported. They exhibit a systematic variation of architectures with 1D chain, 2D sheet, or 3D interpenetrating network. Interestingly, complexes **4** and **5** being isostructural but not isoelectronic species present different magnetic properties.

Experimental

Materials and Methods

1,4-Bis(imidazol-1-yl)benzene, 2,2',5,5'-biphenyltetracarboxylic acid, 3,3',5,5'-biphenyltetracarboxylic acid, and 3,3',4,4'-biphenyltetracarboxylic acid are received from Jinan Camolai Trading Company, China. Other reagents and solvents were obtained from commercial sources and used without further purification. Powder X-ray diffraction (XRD) data were collected on a Miniflex-Rigaku II diffractometer with Cu K α radiation ($\lambda = 1.5418$ Å). The carbon, nitrogen, and hydrogen contents of the complexes were determined by CHNO-Rapid instrument. IR spectra of the compounds were recorded within the 4000–400 cm^{-1} region on a BRUKER TENSOR27 spectrometer with KBr disks. Thermogravimetric (TG) studies were carried out on a Dupont thermal analyzer with temperature range 25–800 °C under air flow with a heating rate of 5 °C min^{-1} . Magnetic susceptibility measurements data were performed by a MPMS RSO Measurement in the temperature range of 1.8–300 K by using an applied field of 2000 Oe. All magnetic data have been corrected for diamagnetism by using Pascal's constants.

Synthesis of compounds 1–5

$[Ni_2(1,4\text{-bib})_3(o,m\text{-bpta})(H_2O)_2]$ (**1**). A mixture of 1,4-bib (0.20 mmol, 0.042 g), $H_4(o,m\text{-bpta})$ (0.10 mmol, 0.033 g), nickel(II) nitrate hexahydrate (0.20 mmol, 0.048 g), KOH (0.30 mmol, 0.0168 g) in 6 ml of H_2O/DMF (5:1 volume ratio) was

placed in a Teflon-lined stainless steel vessel, heated to 160 °C for 3 days, followed by slow cooling to room temperature. Green block crystals of **1** were obtained. Yield of 69% (based on Ni). Element Anal.(%, EA) Calcd. for $C_{52}H_{40}N_{12}O_{10}Ni_2$: C 56.35, H 3.46, N 15.17. Found: C 56.47, H 3.34, N 14.98. IR (cm^{-1} , vs for very strong, s strong, m medium, w weak): 3125.66m, 1586.70vs, 1532.00vs, 1386.73s, 1269.53m, 1134.90w, 1074.92m, 960.92s, 961.83w, 827.02m, 790.18w, 658.39w.

$[Ni_2(1,4\text{-bib})_3(HCO_2)_4(H_2O)_2] \cdot 5H_2O$ (**2**). A mixture of 1,4-bib (0.20 mmol, 0.042 g), $H_4(m,m\text{-bpta})$ (0.10 mmol, 0.033 g), nickel(II) nitrate hexahydrate (0.20 mmol, 0.058 g) in 8.0 ml of H_2O/DMF (3:2 volume ratio) was placed in a Teflon-lined stainless steel vessel, heated to 160 °C for 3 days. After the mixture was slowly cooled to room temperature, green block crystals of **2** were obtained. Yield of 78% (based on Ni). EA(%) Calcd. for $C_{40}H_{34}N_{12}O_{16}Ni_2$: C 45.57, H 4.59, N 15.94. Found: C 45.48, H 4.71, N 15.76. IR (cm^{-1}): 3244.61s, 1626.26vs, 1532.19vs, 1407.57vs, 1360.56s, 1061.21m, 959.35m, 829.80s, 782.07m, 655.50m, 617.98w, 526.10w.

$[Co_2(1,4\text{-bib})_2(m,m\text{-bpta})(H_2O)_4]$ (**3**). The same synthetic procedure as for **3** was used except that cobalt(II) nitrate hexahydrate was replaced by nickel(II) nitrate hexahydrate, giving pink block crystals of **3**. Yield of 36% (based on Co). EA(%) Calcd. for $C_{40}H_{34}N_8O_{12}Co_2$: C 51.29, H 3.66, N 11.96. Found: C 51.06, H 3.58, N 11.72. IR (cm^{-1}): 3233.57s, 3149.14s, 1629.62vs, 1530.48vs, 1448.31s, 1410.03vs, 1356.27vs, 1056.61s, 831.84s, 707.19s.

$[Ni_2(1,4\text{-bib})_2(m,p\text{-bpta})(H_2O)_2]$ (**4**). A mixture of 1,4-bib (0.20 mmol, 0.042 g), $H_4(m,p\text{-bpta})$ (0.10 mmol, 0.033 g), nickel(II) nitrate hexahydrate (0.20 mmol, 0.058 g), and 13 mL of H_2O was placed in a Teflon-lined stainless steel vessel, heated to 160 °C for 3 days, followed by slow cooling to room temperature, giving green block crystals of **4**. Yield of 78% (based on Ni). EA(%) Calcd. for $C_{40}H_{30}N_8O_{10}Ni_2$: C 53.37, H 3.36, N 12.45. Found: C 52.74, H 3.41, N 12.30. IR (cm^{-1}): 3107.99vs, 1607.17vs, 1529.18vs, 1388.67vs, 1320.92s, 1247.11m, 1068.12s, 834.79m, 653.01w, 538.59w.

$[Co_2(1,4\text{-bib})_2(m,p\text{-bpta})(H_2O)_2]$ (**5**). This complex was prepared in procedure to **4** except that nickel(II) nitrate hexahydrate was replaced by cobalt(II) nitrate hexahydrate, giving pink block crystals of **5**. Yield of 53% (based on Co). EA(%) Calcd. for $C_{40}H_{30}N_8O_{10}Co_2$: C 53.35, H 3.36, N 12.44. Found: C 53.40, H 3.39, N 12.41. IR (cm^{-1}): 3117.46vs, 1562.41vs, 1532.47vs, 1398.65vs, 1252.65s, 1072.04s, 962.56m, 833.55m, 661.02w, 551.90w.

X-ray Crystallography

Diffraction data were collected on a Bruker Smart Apex II with a CCD area detector diffractometer Mo-K α ($\lambda = 0.71073$ Å) at room temperature. Absorption corrections were applied by using the multi-scan program SADABS.²¹ The structures were

ARTICLE

Table 1 Crystal Data and Structure Refinement Parameters for Compounds 1–5

Compound	1	2	3	4	5
CCDC	999236	999235	999234	999233	999232
Formula	C ₅₂ H ₄₀ N ₁₂ O ₁₀ Ni ₂	C ₄₀ H ₄₈ N ₁₂ O ₁₅ Ni ₂	C ₄₀ H ₃₄ N ₈ O ₃ Co ₂	C ₄₀ H ₃₀ N ₈ O ₁₀ Ni ₂	C ₄₀ H ₃₀ N ₈ O ₁₀ Co ₂
Fw	1110.38	1054.32	936.62	900.14	900.58
Temp (K)	298(2)	298(2)	298(2)	298(2)	298(2)
Wavelength(Å)	0.71073	0.71073	0.71073	0.71073	0.71073
Size	0.15×0.1×0.1	0.22×0.19×0.15	0.3×0.25×0.25	0.25×0.20×0.20	0.30×0.20×0.15
Crystal system	Monoclinic	Monoclinic	Monoclinic	Triclinic	Triclinic
Space group	<i>C2/c</i>	<i>C2/c</i>	<i>P2₁/c</i>	<i>P-1</i>	<i>P-1</i>
<i>a</i> (Å)	24.579(5)	24.344(1)	11.065(2)	8.159(2)	8.157(3)
<i>b</i> (Å)	11.834(2)	12.291(4)	12.609(2)	9.341(1)	9.405(4)
<i>c</i> (Å)	18.816(3)	18.868(8)	15.087(2)	12.734(1)	12.802(8)
α (°)	90	90	90	105.254(2)	105.220(8)
β (°)	121.090(5)	121.3369(10)	119.371(8)	98.139(2)	98.276(8)
γ (°)	90	90	90	107.777(2)	107.826(6)
Vol (Å ³)	4686.8(1)	4820(3)	1834.4(4)	865.2(2)	874.9(7)
<i>Z</i>	4	4	2	1	1
<i>D_c</i> (g/cm ³)	1.574	1.453	1.696	1.728	1.709
μ (mm ⁻¹)	0.881	0.859	0.987	1.167	1.026
<i>F</i> (000)	2288	2192	960	462	460
<i>R</i> ₁ , <i>wR</i> ₂ [<i>I</i> > 2 σ (<i>I</i>)]	0.0751, 0.2206	0.0583, 0.1464	0.0402, 0.0722	0.0592, 0.1375	0.0324, 0.0699
<i>R</i> ₁ , <i>wR</i> ₂ (all data)	0.1322, 0.2673	0.1017, 0.1743	0.0770, 0.0854	0.1183, 0.1717	0.0445, 0.0751
<i>GOF</i> on <i>F</i> ₂	0.997	1.028	1.011	0.851	1.053
$\rho_{\max, \min}$ (e Å ⁻³)	0.849, -0.570	0.891, -0.323	0.284, -0.320	0.571, -0.605	0.311, -0.338

$$R_1 = \sum \frac{|F_o| - |F_c|}{|F_o|}, \quad wR_2 = \sqrt{\frac{\sum w(F_o^2 - F_c^2)^2}{\sum w(F_o^2)^2}}$$

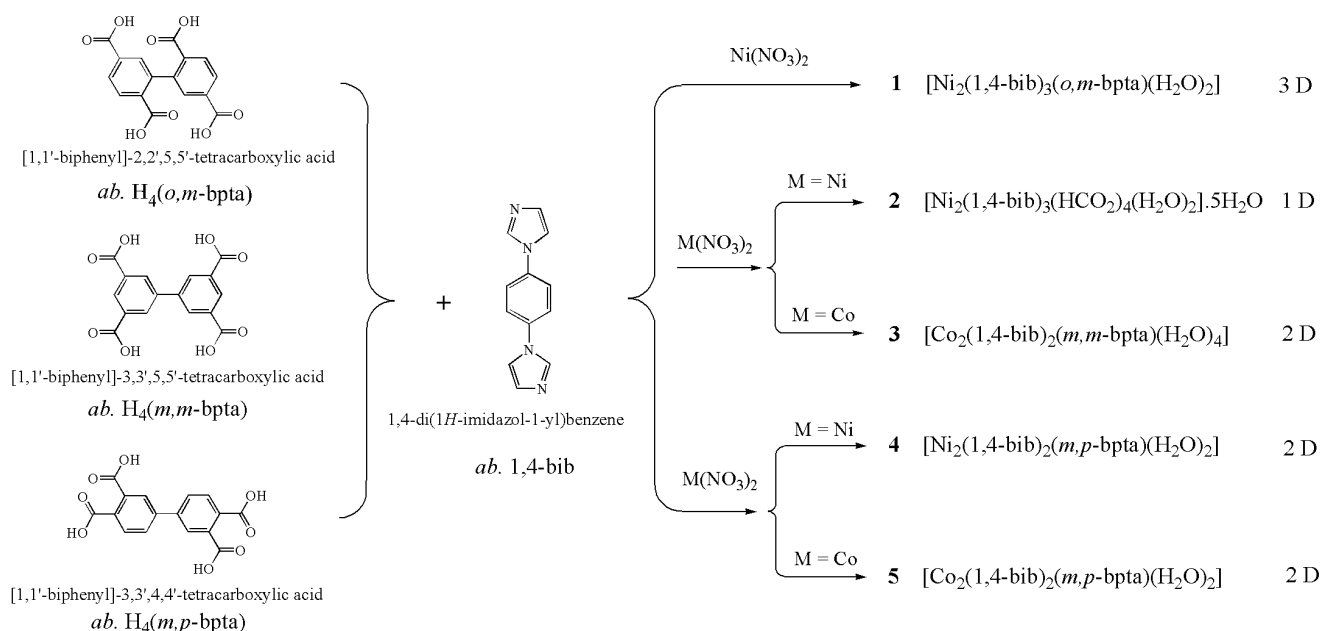
solved by the direct methods and refined by the full-matrix least-squares technique using the SHELXS-97.²² All non-hydrogen atoms were refined anisotropically. Hydrogen atoms attached C were generated geometrically. H atoms of water molecules were located from difference Fourier maps and refined from their global *U*_{iso} values. The detailed

crystallographic data and structure refinement parameters for the compounds are summarized in Table 1.

Results and discussion

Synthesis and Characterization

ARTICLE



Scheme 1 Schematic drawing of 1,4-bib and H₄bptas, as well as the self-assembly process of **1-5**

The self-assembly processes of complexes **1-5** were achieved from Scheme 1. Namely, they were obtained from 1,4-bib and H₄bptas reacting with the nickel/cobalt salts under hydrothermal and solvothermal conditions. In general, the coordination polymers were crystallized to accord with designing routes except complex **2** being gotten from hydrolysis of DMF. The IR spectra of the compounds **1-5** and ligands are shown in the Supporting Information (Figure S1). The infrared absorption spectra showed that the broad band in the range of 3500–3200 cm⁻¹ (3269 cm⁻¹ for **1**, 3232 cm⁻¹ for **2**, 3230 cm⁻¹ for **3**, 3409 cm⁻¹ for **4**, and 3423 cm⁻¹ for **5**) indicate O–H stretching of the coordinated water molecules. The strong absorption peaks located at 1305 cm⁻¹ (1318 cm⁻¹ for **1**, 1412 cm⁻¹ for **2**, 1320 cm⁻¹ for **3**, 1324 cm⁻¹ for **4**, and 1328 cm⁻¹ for **5**) should be attributed the C=N stretching vibration of the 1,4-bib. The characteristic bands of the carboxylate groups in **1-5** appeared in the region at 1629–1527 cm⁻¹. Furthermore, The values occur red-shifted relative to the carboxylate group of H₄bptas and formate ligands, which are consistent with their structural features from the results of crystal structures.

Description of the Crystal Structures

{[Ni₂(1,4-bib)₃(*o,m*-bpta)(H₂O)₂]}_n (1**). Complex **1** crystallizes in the monoclinic space group *C*_{2/c}, with an independent Ni(II) ion, a half fully deprotonated *o,m*-bpta⁴⁻ ligand, one and half 1,4-bib ligands and one coordinated water molecule in the asymmetric unit. As shown in Figure 1a, the six coordinated geometry also can be described as a slightly distorted octahedron with coordination angles in the range of 84.5(2)°–179.8(1)°. The basal positions are occupied by three oxygen atoms (O1, O2, & O5) from one carboxylic group adopting μ₁-η¹:η¹ and one coordinated water molecule, as well as one nitrogen atom (N5) from 1,4-bib ligand. The apical positions are occupied by two nitrogen atoms (N1, & N4B, symmetry code: B -1/2+x, 1/2+y, z) from two 1,4-bib ligands. The Ni–O and Ni–N bond lengths are in the range of 2.06(3)–2.18(1) Å and 2.06(1)–2.08(4) Å, respectively, comparable with those of Ni(II) complexes.^{15c,23} As shown in Figure 1b, four Ni(II) centers are linked by 1,4-bib ligands to yield a rhombic loop with Ni···Ni separation of 13.577(2) and 13.640(2) Å, respectively. Finally, these [Ni₄(1,4-bib)₄] loops are further connected by *o,m*-bpta⁴⁻ ligands to generate a 3D framework with A and B channels viewed toward *b* axis directions. Scrutinizing the crystal structure reveals that the alternate arrangement of the helical chains along *a* axis exists over a 2D layer and all helical chains in a 2D sheet have the**

ARTICLE

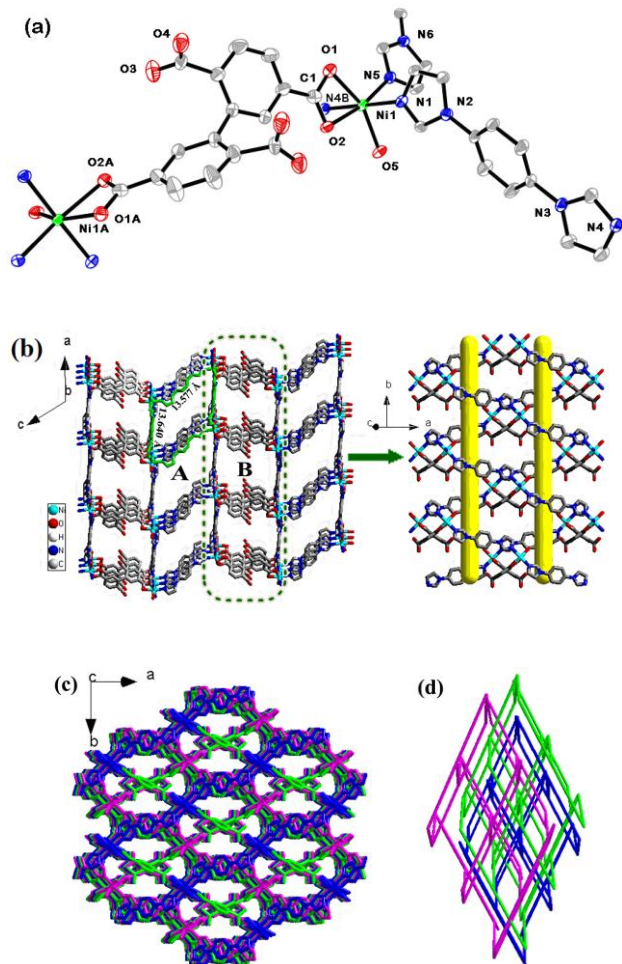


Figure 1 A description of the structure of **1**: (a) The coordination environment of Ni(II) ions. H atoms were omitted for clarity (Symmetry codes: A $-x, y, -1/2-z$; B $-1/2+x, 1/2+y, z$). (b) View of the 2D layer along the *a* axis. (c) The 3D interpenetration network structure. (d) Schematic representation of 3-fold interpenetrating 3D 4-connected net of **1**.

same handedness. The Ni(II) ions are linked to form infinite Ni-1,4-bib-Ni-(*o,m*-bpta⁴⁻)-Ni helical chain with a pitch of 11.834(2). The polymeric Ni(II) coordination framework of the complex **1** displays a unique 3D entangling arrangement with 3-fold interpenetration of the nets (Figure 1c). In isolation, the network topology could be described as having the 4-connected network with the Schläfli notation of $(4.6^2)^2(4^2.6^2.8^2)$. The most interesting structural feature of **1** is that three such networks interpenetrate in a (3D/3D) parallel fashion give rise to a 3D polythreading network (Figure 1d).²⁴

$\{[\text{Ni}_2(\text{1,4-bib})_3(\text{HCO}_2)_4(\text{H}_2\text{O})_2] \cdot 5\text{H}_2\text{O}\}_n$ (**2**). Ligand $\text{H}_4(m,m\text{-bpta})$, was employed in the prescription of synthesis,

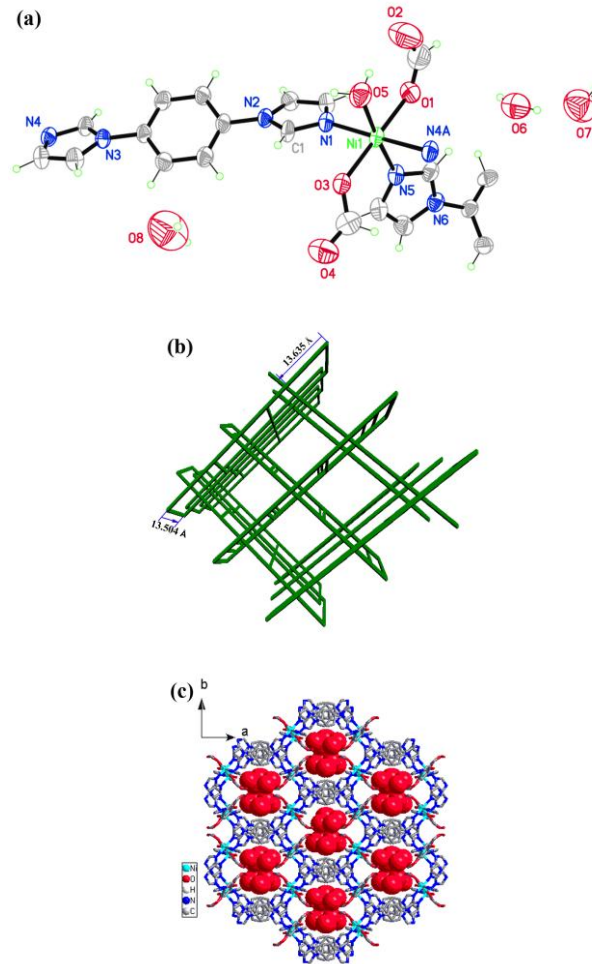


Figure 2 A description of the structure of **2**: (a) The coordination environment of Co(II) atoms. (Symmetry code: A $1/2+x, -1/2+y, z$). (b) View of the 1D ladder-like chain interpenetration structure along the *c* axis. (c) The 3D honeycomb framework with channels via interpenetration. The red balls show the lattice water molecules.

but it was replaced by formate groups in the products. The formate derives from hydrolysis of DMF.²⁵ Thus, a new compound **2** with a distinct 1D ladder-like chain interpenetration structure was obtained. The asymmetric unit consists of one crystallographically independent Ni(II) ion, two COO⁻ anions, one and half 1,4-bib ligands, and some water molecules. Each Ni(II) center in **2** also adopts a octahedral coordination geometry made up of three nitrogen atoms(N1, N5 & N4A, symmetry code: A $1/2+x, -1/2+y, z$) of three 1,4-bib ligands and three oxygen atoms(O1, O3, & O5) from two COO⁻ anions and one coordination water molecule (Figure 2a). Four 1,4-bib ligands connect four Ni(II) ions

forming a $[\text{Ni}_4(1,4\text{-bib})_4]$ parallelogram unit with Ni...Ni separation of 13.504(6) and 13.635(4) Å (Figure 2b), respectively. These parallelograms are linked with each other by the 1, 4-bib ligands forming a linear 1D infinite ladder type chain parallel to the crystallographic plane (66-1). In the crystal packing, these chains are strongly binded with each other *via* the terminal water molecules and the carboxyl oxygen with O...O distances of 2.704(7) Å and form 2D plane supramolecular network. The layers are stacked and interlocked with the two nearest neighboring ones (Figure 2b). Ultimately, these 1D ladder type chains are mutual interpenetration with independent frameworks forming a 1D + 1D → 3D fascinating honeycomb framework with prismatic channels viewed along the *c* axis.²⁶ Despite interpenetration, there are still enough void spaces in the structure occupied by water molecules as guests (Figure 2c). PLATON calculations²⁷ after the removal of the guest molecules show that the guest accessible volume (912.7 Å³ per unit cell) comprises 18.9% of the unit cell volume.

$\{[\text{Co}_2(1,4\text{-bib})_2(m,m\text{-bpta})(\text{H}_2\text{O})_4]\}_n$ (**3**). The crystal structure analysis reveals that complex **3** crystallizes in the monoclinic system with $P2_1/c$ space group. The asymmetric unit possesses one crystallographically independent Co(II) ion, a half of completely deprotonated $m,m\text{-bpta}^{4-}$ ligand, one 1,4-bib ligand, and two coordinated water molecules. As shown in Figure 3a, both Co(II) centers have distorted octahedral geometries and are bridged by two carboxylic groups with $\mu_{1,3}\text{-O}_2\text{O}$ modes, the equatorial plane of which comprises four oxygen atoms (O1, O5, O6 & O2B, symmetry code: B $1-x, 2-y, 2-z$) from two equivalent $m,m\text{-bpta}^{4-}$ anions and two terminal coordination water molecules; two nitrogen atoms (N1 & N4A, symmetry code: A $x+1, y, z+1$) from two 1,4-bib ligands occupying the apical sites. The Co–O and Co–N distances are in the ranges of 2.041(2)–2.179(2) and 2.109(3)–2.146(3) Å, respectively. The carboxylic groups of $m,m\text{-bpta}^{4-}$ ligands in **3** are completely deprotonated and exhibit $\mu_2\text{-}\eta^1\text{:}\eta^1$ coordination modes to bond four Co(II) ions. Two carboxylic groups bridge two Co(II) centers to form a 8-membered $\text{Co}_2(\text{CO}_2)_2$ ring structure unit with the Co...Co distance of 4.388(1) Å, which generates a 1D chain in the direction of *b*-axis. The Co...Co distance is slightly longer than the previously reported analogous complexes.²⁸ The 1D chain is further linked by 1,4-bib spacers resulting in the formation of a final complicated 2D square grids (Figure 3b), which are finally assembled into a 3D framework via hydrogen bonds (Figure 3c). From a topological perspective, the complex **3** can be simplified as 4-connected square planar nodes (Figure 3d).

$\{[\text{Ni}_2(1,4\text{-bib})_2(m,p\text{-bpta})(\text{H}_2\text{O})_2]\}_n$ (**4**) and $\{[\text{Co}_2(1,4\text{-bib})_2(m,p\text{-bpta})(\text{H}_2\text{O})_2]\}_n$ (**5**). The single-crystal X-ray diffraction data report that compounds **4** & **5** are isomorphism and crystallize in the triclinic system with space group $P\bar{1}$, herein, only the structure of **5** is discussed as a representation.

As shown in Figure 4a, Co(II) ion is hexa-coordinated with one terminal coordination water molecule (O5) and three O

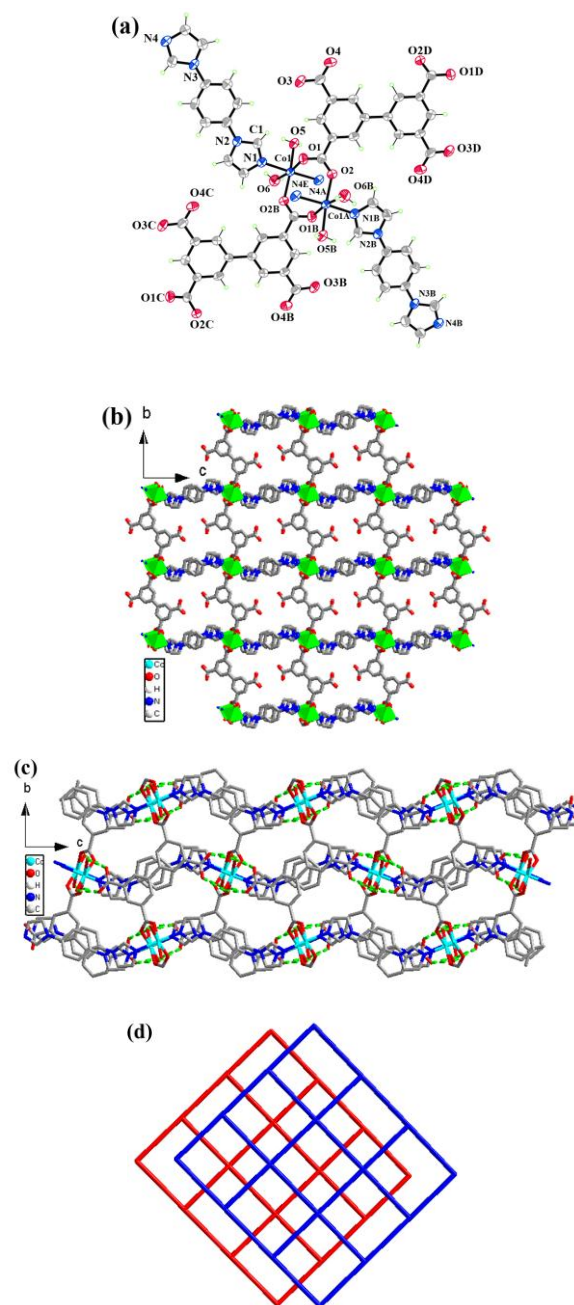


Figure 3 A description of the structure of **3**: (a) The coordination environment of Co(II) ions. (Symmetry codes: A $x+1, y, z+1$; B $1-x, 2-y, 2-z$; C $x, y+1, z$; D $1-x, 1-y, 2-z$; E $-x, 2-y, 1-z$) (b) View of the 2D sheet with square grids along the *a* axis. (c) Infinite 3D framework assembled from hydrogen bonds viewed along the *a* axis. (d) (4, 4)-connected 2D layers for **3**.

atoms (O1, O1A & O3A) from the carboxyl of $m,p\text{-bpta}^{4-}$ ligand and two nitrogen atoms (N1 & N4C) from two 1,4-bib ligands to form a slightly distorted octahedral coordination geometry, and O1, O1A, O3A and O5 compose the equatorial plane, while N1 and N4C at the axial site. The Co–O and Co–N distances are in the ranges of 2.061(3)–2.171(3) and 2.133(2)–2.146(2) Å, respectively, which are all within the reported values of Co(II) complexes.^{17a, 29} Each deprotonated

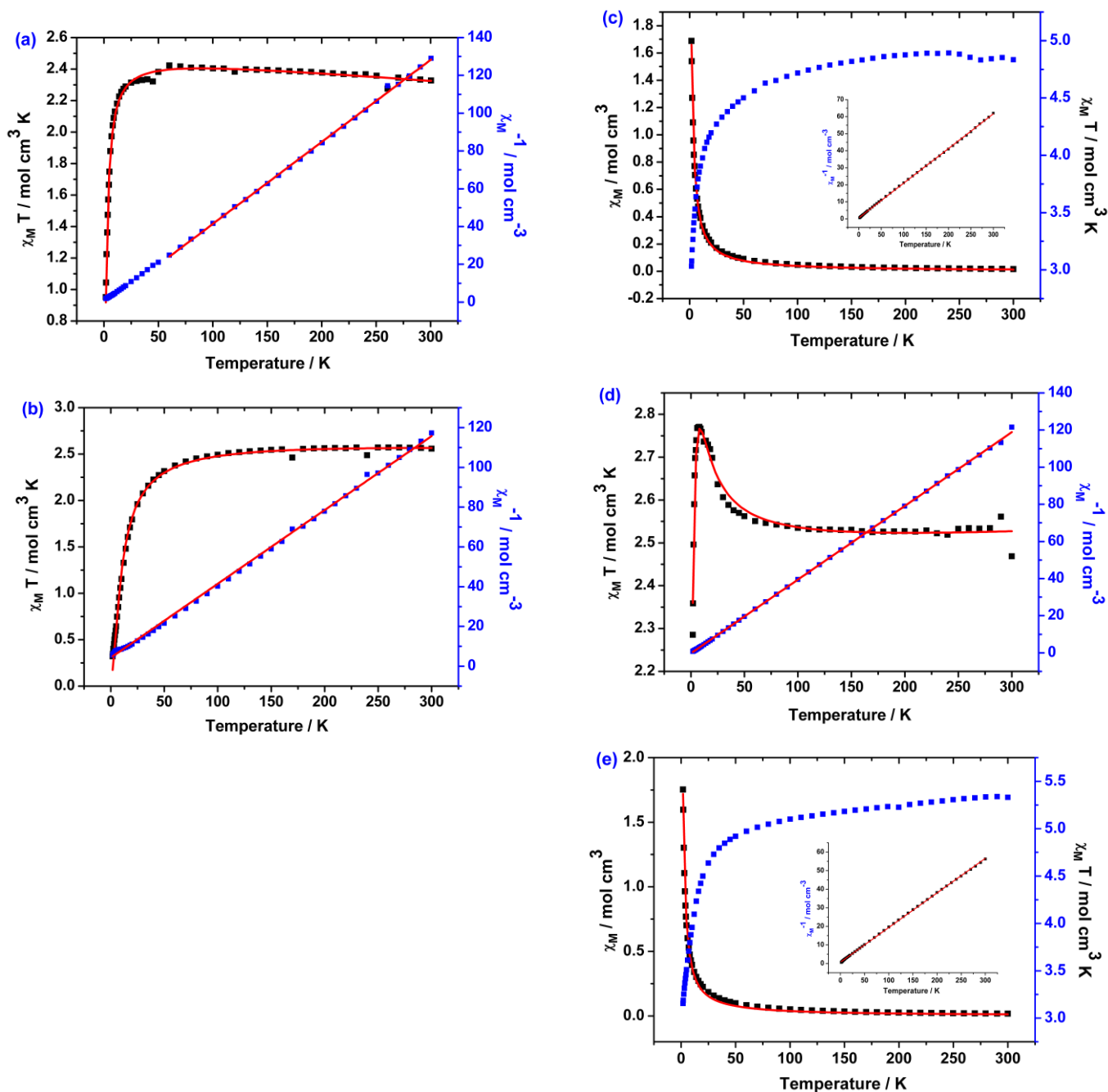


Figure 5 Temperature dependence of $\chi_M T$ and $1/\chi_M$ collected in an applied field of 0.2 T for compound (a) **1**, (b) **2**, (c) **3**, (d) **4**, and (e) **5**.

magnetic data can be properly fitted using the following equation, where N , g , β , and k have their usual meanings and $x = J/kT$.

$$\chi_{chain} = \frac{N\beta^2 g^2}{kT} \left[\frac{(2.0 + 0.019x + 0.777x^2)}{(3.0 + 4.346x + 3.232x^2 + 5.834x^3)} \right] \quad (1)$$

Eqn. (1) has been modified to (2) to include the molecular-field approximation and temperature in dependent paramagnetism ($N\alpha$).

$$\chi_M = \frac{\chi_{chain}}{[1 - (zJ'/N\beta^2 g^2)\chi_{chain}]} + 2N_a \quad (2)$$

The best simulated values are $g = 2.235(5)$, $J = 0.906(1) \text{ cm}^{-1}$, $zJ' = 0.084(1) \text{ cm}^{-1}$ and $R = 3.79 \times 10^{-3}$. The moderately positive θ value and the small $J > 0$ value indicating the presence of a weak ferromagnetic exchange between adjacent Ni(II) centers in **1**.

For **2**, the experimental $\chi_M T$ value $2.56 \text{ cm}^3 \text{ mol}^{-1} \text{ K}$ at 300 K is higher than the expected spin-only value of $2.0 \text{ cm}^3 \text{ mol}^{-1} \text{ K}$ for isolated $[\text{Ni(II)}]_2$ ions due to the orbital contribution to the magnetic moment. As the temperature is lowered from 300 K, the $\chi_M T$ value gradually drops to $0.32 \text{ cm}^3 \text{ mol}^{-1} \text{ K}$ at 1.8 K. The molar magnetic susceptibility rang from 300 to 1.8 K obeys the Curie–Weiss law with $C = 2.703 \text{ cm}^3 \text{ mol}^{-1} \text{ K}$ and $\theta = -11.62 \text{ K}$. The negative Weiss constant and the decrease of $\chi_M T$ with a decrease of the temperature can be referred to the presence of typical antiferromagnetic interaction among adjacent Ni(II) ions. Ni(II) ions are bridged by the 1, 4-bib ligand forming a linear 1D infinite chain. To quantify magnetic interaction behavior, the magnetic data were fit with the above Eqn. (1) over the entire temperature rang. The best fit values were $g = 2.327(4)$ and $J = -3.877(1) \text{ cm}^{-1}$, with $R = 3.3 \times 10^{-3}$; The negative J value indicates that there is weak antiferromagnetic interaction between adjacent Ni(II) centers.

The $\chi_M T$ values of **3** and **5** at room temperature are 4.83 and $5.33 \text{ cm}^3 \text{ K mol}^{-1}$, respectively, considerably larger than expected value of $3.75 \text{ cm}^3 \text{ K mol}^{-1}$ for the spin only value of two uncoupled Co(II) ions with $S = 3/2$ ion and $g = 2.0$. Along the cooling temperature, the values of $\chi_M T$ slightly decrease and then fall very rapidly below 70 K to reach 3.03 and $3.16 \text{ cm}^3 \text{ K mol}^{-1}$ at 1.8 K, respectively. This smoothly decrease indicates the occurrence of antiferromagnetic coupling. The decrease at high temperature should be due to a larger orbital contribution arising from the $^4T_{1g}$ ground state of Co(II). Fitting of the $1/\chi_M$ vs T data using the Curie–Weiss law (1.8–300 K) obtained the value for $C = 4.912$ and $5.362 \text{ cm}^3 \text{ K mol}^{-1}$ and $\theta = -2.824$ and -3.631 K for **3** and **5**, respectively. From the magnetic point of view, the Co...Co distances in complexes **3** and **5** are very close ranges. The distances of 1,4-bib bridging modes are 13.649(2) and 13.752(6) Å, respectively. Synchronously, those of bpta⁴⁻ bridging modes are 12.609(1) and 12.802(8) Å. The long distances of Co...Co both complexes might exclude an efficient direct exchange between the Co(II) ions. From the features of crystal structures of **3** and **5**, there are obviously differences of bridging modes between two Co(II) dimers, namely, $\mu_{1,3}$ -O,O bridges with Co...Co separation of 4.388(1) Å in **3** and $\mu_{1,1}$ -O bridges with relative 3.268(1) Å in **5**. But these distances are very smaller than those of not only 1,4-bib but also bpta⁴⁻ bridges. Thus, we may presume that the main magnetic interactions of both the complexes should mainly limit in $\text{Co}_2(\mu_{1,3}\text{-COO})_2$ and $\text{Co}_2(\mu_{1,1}\text{-COO})_2$ dimers. On account of the distorted

octahedron geometry of the Co(II) center, the spin Hamiltonian of the Co(II) dimer coupling should be written as $\vec{H} = -J\vec{S}_1 \cdot \vec{S}_2$, where J is the intradimer interaction parameter of Co(II) ions. Thus, the magnetic data of **3** and **5** are fitted by Eqn. (3)³⁰:

$$\chi_{dimer} = \frac{2N\beta^2 g^2}{kT} \left[\frac{(e^{-10x} + 5e^{-6x} + 14)}{(e^{-12x} + 3e^{-10x} + 5e^{-6x} + 7)} \right] \quad (3)$$

wherein $x = J/kT$. The least squares fit of the experimental data in the range of 1.8–300 K to the Eqn(3) led to $g = 2.041(1)$, $J = -0.1164(1) \text{ cm}^{-1}$, $R = 1.0 \times 10^{-3}$ for **3** and $g = 2.035(1)$, $J = -0.100(1) \text{ cm}^{-1}$, $R = 2.2 \times 10^{-3}$ for **5**. The facts of $\theta < 0$ and $J < 0$ indicate that there are weak antiferromagnetic interactions between neighboring Co(II) ions for both the complexes.

The field dependence of magnetization (M) for **5** has been determined at 1.8 K in the range of 0–70 KOe (Figure S5 (b)), displaying a gradual increase of the magnetization at low fields, and following with a lack of saturation even at 70 KOe. The phenomenon indicate the present of antiferromagnetic interactions among adjacent Co(II) ions.

The $\chi_M T$ value of **4** per Ni(II)₂ unit is $2.468 \text{ cm}^3 \text{ K mol}^{-1}$ at 300 K, which is also larger than the spin only value of two uncoupled Ni(II) ions ($2.0 \text{ cm}^3 \text{ K mol}^{-1}$) with $S = 1$ and $g = 2.00$. Upon cooling, the $\chi_M T$ values increase smoothly and reaches a maximum $2.77 \text{ cm}^3 \text{ K mol}^{-1}$ at 8 K, which indicates a characteristic feature of ferromagnetic coupling between Ni(II) ions. Below 8 K, the $\chi_M T$ value decreases abruptly to $2.29 \text{ cm}^3 \text{ K mol}^{-1}$ at 1.8 K. The sharp decrease of the $\chi_M T$ value at a very low temperature region may be attributed to either a zero-field splitting factor or interdimer antiferromagnetic interactions.

The Curies–weiss fit in the range of 1.8 to 300 K affords Curie constant of $C = 2.518 \text{ cm}^3 \text{ K mol}^{-1}$ and a Weiss constant of $\theta = 0.677 \text{ K}$. In **4**, the metal center distance of Ni₂(CO₂)₂ units is 3.229(1) Å, and the Ni...Ni distances through the 1,4-bib and (m,p)bpta⁴⁻ linked are 13.668(2) and 13.336(2) Å, respectively. The coupling interactions of the longer distances are negligible for magnetic exchange between the Ni(II) ions. Thus, the dimer model was used to analyze the magnetic data. The hamiltonian describing the situation of the dimer is given as $\vec{H} = -J\vec{S}_1 \cdot \vec{S}_2$. The expression of magnetic susceptibility, derived from the Hamiltonian, is given in Eqn (4)³¹:

$$\chi_{dimer} = \frac{Ng^2\beta^2}{kT} \frac{1 + 5\exp(4J/kT)}{3 + 5\exp(4J/kT) + \exp(-2J/kT)} \quad (4)$$

The interdimer interaction (zJ') was accounted for by the molecular-field approximation:

$$\chi_M = \frac{\chi_{dimer}}{1 - (zJ'/N\beta^2 g^2)\chi_{dimer}} + \frac{Ng^2\beta^2}{3kT} S(S+1) + N_a \quad (5)$$

In the Eqn (5), the second item is the contribution of the isolated Ni(II) ions. The best-fit parameters obtained from minimizing R were $g = 2.223(7)$, $J = 2.220(1) \text{ cm}^{-1}$, $zJ' = -0.807(1) \text{ cm}^{-1}$, and $R = 4.749(1) \times 10^{-4}$. The g value is also in accord with expectation for Ni(II) complexes.³² The positive θ and J values indicate the presence of weak ferromagnetic interaction between Ni(II) ions.

For **4**, the saturated magnetization of $4.09 N\beta$ per Ni_2 unit at the highest field of 70 KOe is close to the expected value of $4.0 N\beta$ for two ferromagnetic Ni(II) ions (Figure S5 (a)). The observed ferromagnetic interactions should be mainly from a magnetic exchange through the O atom bridges.

Visibly, the magnetic properties of the complex **4** is different from those of the complex **5**, although they are isostructural in crystal structures. To our knowledge, the magnetic properties of a complex mostly come from the electronic species of metal and non-metal as well as their bond modes. In our examples, both the complexes have same bridging modes ($\mu_{1,1}\text{-COO}$) with the close M-O-M angles and M...M distances in **4** ($100.3(2)^\circ$, $3.229(1) \text{ \AA}$) and **5** ($99.7(1)$, $3.268(1) \text{ \AA}$) and different metal ions (Ni(II) and Co(II)), which is not isoelectronic species. Further evaluation of this difference might come from the method of neutron diffraction.

Conclusions

In conclusion, we have successfully constructed five novel coordination polymers with different network structures from the different biphenyltetracarboxylate ligands under the similar synthetic procedure. Compound **1** is a 3D framework with 3-fold interpenetration. In addition, compound **2** is a 1D structure with mutual interpenetration chains due to $\text{H4}(m,m\text{-bpta})$ ligand decomposed into the COO^- anion. Compounds **3–5** are all 2D motifs, which are joined via H-bond bridges to give different 3D supramolecular architectures. The variable attachment position of carboxylic groups plays a vital role in the formation of the different structures. Magnetic studies indicate the presence of a weak ferromagnetic exchange for **1** and **4**, and antiferromagnetic behavior for the compounds **2**, **3** and **5**. We are currently working with such polycarboxylate compounds to explore the fascinating structure and properties in our laboratory.

Acknowledgements

We gratefully acknowledge the financial support of the Natural Science Foundation of China (Grant Nos. 21171109, 21271121, and 201201113), SRFDP (Grant Nos. 20111401110002, 20111401120001, and 20121401110005), the Provincial Natural Science Foundation of Shanxi Province of China (Grant Nos. 2011011009-1) and the Shanxi Scholarship Council of China (2012-004) for financial support.

References

- (a) J.-P. Zhang, Y.-B. Zhang, J.-B. Lin and X.-M. Chen, *Chem. Rev.*, 2012, **112**, 1001; (b) A. Betard and R. A. Fischer, *Chem. Rev.*, 2012, **112**, 1055; (c) S. M. Cohen, *Chem. Rev.*, 2012, **112**, 970; (d) J. An, C. M. Shade, D. A. Chengelis-Czegan, S. Petoud and N. L. Rosi, *J. Am. Chem. Soc.*, 2011, **133**, 1220; (e) Y. Kubota, M. Takata, R. Matsuda, R. Kitaura, S. Kitagawa and T. C. Kobayashi, *Angew. Chem., Int. Ed.*, 2006, **45**, 4932; (f) T. K. Maji, R. Mastuda and S. Kitagawa, *Nat. Mater.*, 2007, **6**, 142.
- (a) O. Shekhah, H. Wang, M. Paradinas, C. Ocal, B. Schupbach, A. Terfort, D. Zacher, R. A. Fischer and C. Woll, *Nat. Mater.*, 2009, **8**, 481; (b) S. Bureekaew, H. Sato, R. Matsuda, Y. Kubota, R. Hirose, J. Kim, K. Kato, M. Takata and S. Kitagawa, *Angew. Chem., Int. Ed.*, 2010, **49**, 7660; (c) H. Wu, J. Yang, Z.-M. Su, S. R. Batten and J.-F. Ma, *J. Am. Chem. Soc.*, 2011, **133**, 11406; (d) M. O'Keeffe and O. M. Yaghi, *Chem. Rev.*, 2012, **112**, 675; (e) N. Stock and S. Biswas, *Chem. Rev.*, 2012, **112**, 933; (f) J. I. Feldblyum, D. Dutta, A. G. Wong-Foy, A. Dailly, J. Imirzian, D. W. Gidley and A. J. Matzger, *Langmuir*, 2013, **29**, 8146; (g) L. Fan, X. Zhang, Z. Sun, W. Zhang, Y. Ding, W. Fan, L. Sun, X. Zhao and H. Lei, *Cryst. Growth Des.*, 2013, **13**, 2462.
- (a) H. Amouri, C. Desmarests and J. Moussa, *Chem. Rev.*, 2012, **112**, 2015; (b) M. Yoon, R. Srirambalaji and K. Kim, *Chem. Rev.*, 2012, **112**, 1196; (c) A. B. Sorokin, *Chem. Rev.*, 2013, **113**, 8152.
- (a) Y. Yan, S. Yang, A. J. Blake, W. Lewis, E. Poirier, S. A. Barnett, N. R. Champness and M. Schroder, *Chem. Commun.*, 2011, **47**, 9995; (b) M. P. Suh, H. J. Park, T. K. Prasad and D. W. Lim, *Chem. Rev.*, 2012, **112**, 782; (c) J.-R. Li, J. Sculley and H.-C. Zhou, *Chem. Rev.*, 2012, **112**, 869; (d) B. Yuan, X. Wu, Y. Chen, J. Huang, H. Luo and S. Deng, *Environ. Sci. Technol.*, 2013, **47**, 5474.
- (a) L. Han, M. Hong, R. Wang, J. Luo, Z. Lin and D. Yuan, *Chem. Commun.*, 2003, 2580; (b) Y. Zhou, M. Hong and X. Wu, *Chem. Commun.*, 2006, 135; (c) C. Wang, T. Zhang and W. Lin, *Chem. Rev.*, 2012, **112**, 1084; (d) F. Du, H. Zhang, C. Tian and S. Du, *Cryst. Growth Des.*, 2013, **13**, 1736.
- (a) X.-L. Wang, C. Qin and E.-B. Wang, *Cryst. Growth Des.*, 2006, **6**, 439; (b) A. Corma, H. Garcia and F. X. Llabres i Xamena, *Chem. Rev.*, 2010, **110**, 4606; (c) H.-J. Lu, Y.-Y. Zhu, N. Chen, Y.-C. Gao, X.-F. Guo, G. Li and M.-S. Tang, *Cryst. Growth Des.*, 2011, **11**, 5241; (d) J.-M. Zhou, W. Shi, N. Xu and P. Cheng, *Cryst. Growth Des.*, 2013, **13**, 1218; (e) L. D. Earl, B. O. Patrick and M. O. Wolf, *Inorg. Chem.*, 2013, **52**, 10021.
- (a) C. Serre, C. Mellot-Draznieks, S. Surblé, N. Audebrand, Y. Filinchuk and G. Férey, *Science*, 2007, **315**, 1828; (b) M. B. Andrews and C. L. Cahill, *Chem. Rev.*, 2013, **113**, 1121; (c) L. E. Kreno, K. Leong, O. K. Farha, M. Allendorf, R. P. Van Duyne and J. T. Hupp, *Chem. Rev.*, 2012, **112**, 1105; (d) P. Horcajada, R. Gref, T. Baati, P. K. Allan, G. Maurin, P. Couvreur, G. Férey, R. E. Morris and C. Serre, *Chem. Rev.*, 2012, **112**, 1232; (e) W.-Q. Kan, B. Liu, J. Yang, Y.-Y. Liu and J.-F. Ma, *Cryst. Growth Des.*, 2012, **12**, 2288; (f) G. Férey, *Chem. Soc. Rev.*, 2008, **37**, 191.
- (a) T. R. Cook, Y.-R. Zheng and P. J. Stang, *Chem. Rev.*, 2013, **113**, 734; (b) Y. Cui, Y. Yue, G. Qian and B. Chen, *Chem. Rev.*, 2012, **112**, 1126; (c) J. P. Malrieu, R. Caballol, C. J. Calzado, C. de Graaf and N. Guihery, *Chem. Rev.*, 2014, **114**, 429.
- (a) Y.-H. Chi, J.-M. Shi, H.-N. Li, W. W., E. Cottrill, N. Pan, H. Chen, Y. Liang, L. Yu, Y.-Q. Zhang and C. Hou, *Dalton Trans.*,

- 2013, **42**, 15559; (b) R. D. Willett, C. J. Gómez-García, B. Twamley, S. Gómez-Coca and E. Ruiz, *Inorg. Chem.*, 2012, **51**, 5487.
- 10 (a) E. Coronado, M. Gimenez-Marques and G. Minguez Espallargas, *Inorg Chem.*, 2012, **51**, 4403; (b) R. Y. Li, B. W. Wang, X.-Y. Wang, X.-T. Wang, Z.-M. Wang and S. Gao, *Inorg Chem.*, 2009, **48**, 7174; (c) D. I. Alexandropoulos, L. Cunha-Silva, L. Pham, V. Bekiari, G. Christou and T. C. Stamatatos, *Inorg Chem.*, 2014; (d) A. M. Bryan, G. J. Long, F. Grandjean and P. P. Power, *Inorg Chem.*, 2014, **53**, 2692; (e) F.-P. Huang, J.-L. Tian, W. Gu, X. Liu, S.-P. Yan, D.-Z. Liao and P. Cheng, *Cryst. Growth Des.*, 2010, **10**, 1145; (f) S. Yokota, K. Tsujimoto, S. Hayashi, F. Pointillart, L. Ouahab and H. Fujiwara, *Inorg Chem.*, 2013, **52**, 6543; (g) S. Giri and S. K. Saha, *J. Phys. Chem. Lett.*, 2011, **2**, 1567.
- 11 (a) J.-P. Zhao, S.-D. Han, R. Zhao, Q. Yang, Z. Chang and X.-H. Bu, *Inorg Chem.*, 2013, **52**, 2862; (b) S. I. Vasylevskyy, G. A. Senchyk, A. B. Lysenko, E. B. Rusanov, A. N. Chernega, J. Jezierska, H. Krautscheid, K. V. Domasevitch and A. Ozarowski, *Inorg Chem.*, 2014, **53**, 3642; (c) A. Banisafar, D. P. Martin, J. S. Lucas and R. L. LaDuca, *Cryst. Growth Des.*, 2011, **11**, 1651; (d) H. Li, Y. Han, X. Lv, S. Du, H. Hou and Y. Fan, *CrystEngComm.*, 2013, **15**, 3672.
- 12 (a) J. Ma, F.-L. Jiang, L. Chen, M.-Y. Wu, S.-Q. Zhang, D. Han, R. Feng and M. C. Hong, *Cryst. Growth Des.*, 2011, **11**, 3273; (b) D. Tian, Y. Pang, Y.-H. Zhou, L. Guan and H. Zhang, *CrystEngComm.*, 2011, **13**, 957.
- 13 (a) K. Sumida, M. R. Hill, S. Horike, A. Dailly and J. R. Long, *J. Am. Chem. Soc.*, 2009, **131**, 15120; (b) O. Fabelo, J. Pasán, L. Cañadillas-Delgado, F. S. Delgado, A. Labrador, F. Lloret, M. Julve and C. Ruiz-Pérez, *Cryst. Growth Des.*, 2008, **8**, 3984; (c) Q. Lin, T. Wu, S.-T. Zheng, X. Bu and P. Feng, *Chem. Commun.*, 2011, **47**, 11852; (d) H.-J. Li, Y. Han, X.-F. Lv, S.-S. Du, H.-W. Hou and Y.-T. Fan, *CrystEngComm*, 2013, **15**, 3672.
- 14 (a) P. Holý, J. Závada, I. Císařová and J. Podlaha, *Angew. Chem., Int. Ed.*, 1999, **38**, 381; (b) Z.-R. Pan, J. Xu, X.-Q. Yao, Y.-Z. Li, Z.-J. Guo and H.-G. Zheng, *CrystEngComm*, 2011, **13**, 1617.
- 15 (a) X. Zhang, L. Fan, Z. Sun, W. Zhang, D. Li, J. Dou and L. Han, *Cryst. Growth Des.*, 2013, **13**, 792; (b) J.-J. Wang, L. Gou, H.-M. Hu, Z.-X. Han, D.-S. Li, G.-L. Xue, M.-L. Yang and Q.-Z. Shi, *Cryst. Growth Des.*, 2007, **7**, 1514; (c) D. Tian, Y. Pang, Y.-H. Zhou, L. Guan and H. Zhang, *CrystEngComm*, 2011, **13**, 957.
- 16 (a) T.-H. Park, K. Koh, A. G. Wong-Foy, A. J. Matzger, *Cryst. Growth Des.*, 2011, **11**, 2059; (b) P. K. Yadav, N. Kumari, P. Pachfule, R. Banerjee, L. Mishra, *Cryst. Growth Des.*, 2012, **12**, 5311.
- 17 (a) N. L. Rosi, J. Kim, M. Eddaoudi, B. Chen, M. O'Keeffe and O. M. Yaghi, *J. Am. Chem. Soc.*, 2005, **127**, 1504; (b) P. K. Chen, Y. Qi, Y.-X. Che and J.-M. Zheng, *CrystEngComm*, 2010, **12**, 720; (c) C.-C. Ji, J. Li, Y.-Z. Li, Z.-J. Guo and H.-G. Zheng, *CrystEngComm*, 2011, **13**, 459; (d) L.-H. Cao, Q.-Q. Xu, S.-Q. Zang, H.-W. Hou and T. C. W. Mak, *Cryst. Growth Des.*, 2013, **13**, 1812.
- 18 (a) T.-F. Liu, J. Lu and R. Cao, *CrystEngComm*, 2010, **12**, 660; (b) J. Sahu, M. Ahmad and P. K. Bharadwaj, *Cryst. Growth Des.*, 2013, **13**, 2618; (c) S. Sanda, S. Parshamoni, A. Adhikary and S. Konar, *Cryst. Growth Des.*, 2013, **13**, 5442.
- 19 (a) L. Chen, G.-J. Xu, K.-Z. Shao, Y.-H. Zhao, G.-S. Yang, Y.-Q. Lan, X.-L. Wang, H.-B. Xu and Z.-M. Su, *CrystEngComm.*, 2010, **12**, 2157; (b) Q. Chu, Z. Su, J. Fan, T. Okamura, G.-C. Lv, G.-X. Liu, W.-Y. Sun and N. Ueyama, *Cryst. Growth Des.*, 2011, **11**, 3885; (c) Y. Qi, Y.-X. Che and J.-M. Zheng, *Cryst. Growth Des.*, 2008, **8**, 3602.
- 20 (a) Y.-W. Li, H. Ma, Y.-Q. Cen, K.-H. He, Z.-X. Li and X.-H. Bu, *Cryst. Growth Des.* 2012, **12**, 189; (b) G.-S. Yang, Y.-Q. Lan, H.-Y. Zang, K.-Z. Shao, X.-L. Wang, Z.-M. Su and C.-J. Jiang, *CrystEngComm*, 2009, **11**, 274; (c) J. Fan and B.E.Hanson, *Inorg. Chem.*, 2005, **44**, 6998.
- 21 *SMART, SAINT and SADABS; Bruker AXS Inc.: Madison, Wisconsin, USA*, 1998.
- 22 G. M. Sheldrick, *SHELXS-97, Program for X-ray Crystal Structure Determination*; University of Göttingen: Göttingen, Germany, 1997.
- 23 (a) F. Guo, B. Zhu, M. Liu, X. Zhang, J. Zhang and J. Zhao, *CrystEngComm*, 2013, **15**, 6191; (b) G.-S. Yang, Y.-Q. Lan, H.-Y. Zang, K.-Z. Shao, X.-L. Wang, Z.-M. Su and C.-J. Jiang, *CrystEngComm*, 2009, **11**, 274.
- 24 (a) G.-B. Li, J.-M. Liu, Y.-P. Cai and C.-Y. Su, *Cryst. Growth Des.*, 2011, **11**, 2763; (b) K.-P. Rao, M. Higuchi, J.-G. Duan and S. Kitagawa, *Cryst. Growth Des.*, 2013, **13**, 981; (c) S. Mukherjee, D. Samanta and P. S. Mukherjee, *Cryst. Growth Des.*, 2013, **13**, 5335; (d) X. He, X.-P. Lu, M.-X. Li and R. E. Morris, *Cryst. Growth Des.*, 2013, **13**, 1649.
- 25 (a) Z.-B. Han, Y.-F. Liang, M. Zhou, Y.-R. Zhang, L. Li and J. Tong, *CrystEngComm*, 2012, **14**, 6952; (b) A. D. Burrows, K. Cassar, M. W. F. Richard, M. F. Mahon, S. P. Rigby and J. E. Warren, *CrystEngComm*, 2005, **7**, 548; (c) R.-Q. Zou, A. I. Abdel-Fattah, H.-W. Xu, A. K. Burrell, T. E. Larson, T. M. McCleskey, Q. Wei, M. T. Janicke, D. D. Hickmott, T. V. Timofeeva and Y.-S. Zhao, *Cryst. Growth Des.*, 2010, **10**, 1301; (d) F.-G. Dai, P.-P. Cui, F. Ye and D.-F. Sun, *Cryst. Growth Des.*, 2010, **10**, 1474.
- 26 (a) R. Sen, D. Mal, P. Brandão, R. A. S. Ferreira and Z. Lin, *Cryst. Growth Des.*, 2013, **13**, 5272; (b) D. Sun, L.-L. Han, S. Yuan, Y.-K. Deng, M.-Z. Xu and D.-F. Sun, *Cryst. Growth Des.*, 2013, **13**, 377.
- 27 A. L. Spek, *J. Appl. Crystallogr.*, 2003, **36**, 7.
- 28 Q. Yang, X. Chen, J. Cui, J. Hu, M. Zhang, L. Qin, G. Wang, Q. Lu and H. Zheng, *Cryst. Growth Des.*, 2012, **12**, 4072.
- 29 M. Murrie, *Chem. Soc. Rev.*, 2010, **39**, 1986.
- 30 (a) J. A. Wertz and J. R. Bolton, *Electron paramagnetic resonance: elementary theory and practical applications*, John Wiley & Sons, 2007. (b) Y. Liu, N. Li, L. Li, H.-L. Guo, X.-F. Wang and Z.-X. Li, *CrystEngComm*, 2012, **14**, 2080.
- 31 Y. Liu, N. Li, L. Li, H.-L. Guo, X.-F. Wang and Z.-X. Li, *CrystEngComm*, 2012, **14**, 2086.
- 32 A. Ginsberg, R. Martin, R. Brookes and R. Sherwood, *Inorg. Chem.*, 1972, **11**, 2884.

Graphical Abstract

Self-assembly and Magnetic Properties of Ni(II)/Co(II) Coordination Polymers Based on 1,4-Bis(imidazol-1-yl)benzene and Varying Biphenyltetracarboxylates

*Feng Su^a, Liping Lu^{*a}, Sisi Feng^a, and Miaoli Zhu^{*a,b}*

Five complexes of 1,4-bis(imidazol-1-yl)benzene, H₄bptas and cobalt/nickel are synthesized via solvothermal reaction, both of them with intriguing interpenetrated architectures.

